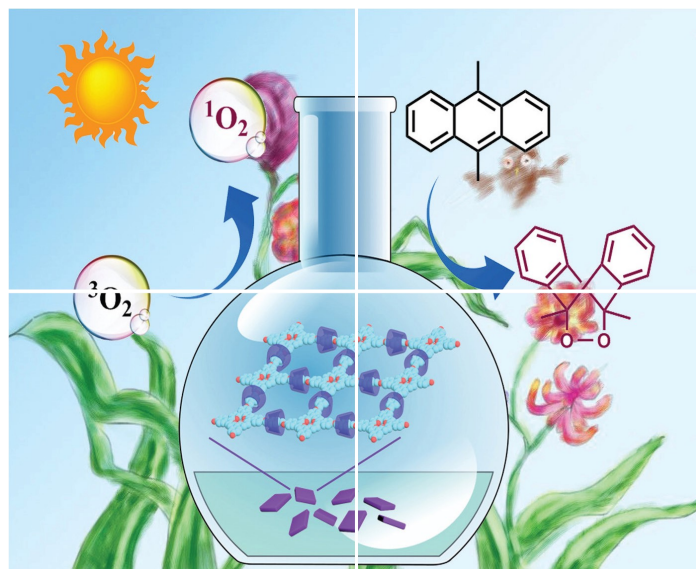


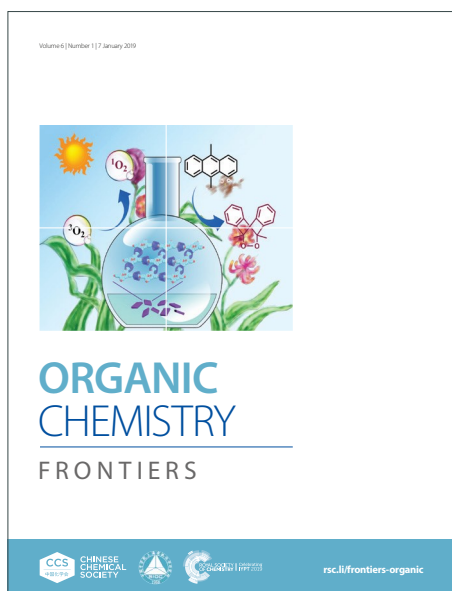
# ORGANIC CHEMISTRY

## FRONTIERS

Accepted Manuscript



This article can be cited before page numbers have been issued, to do this please use: A. Mohapatra and V. Tyagi, *Org. Chem. Front.*, 2026, DOI: 10.1039/D6QO00499G.



This is an Accepted Manuscript, which has been through the Royal Society of Chemistry peer review process and has been accepted for publication.

Accepted Manuscripts are published online shortly after acceptance, before technical editing, formatting and proof reading. Using this free service, authors can make their results available to the community, in citable form, before we publish the edited article. We will replace this Accepted Manuscript with the edited and formatted Advance Article as soon as it is available.

You can find more information about Accepted Manuscripts in the [Information for Authors](#).

Please note that technical editing may introduce minor changes to the text and/or graphics, which may alter content. The journal's standard [Terms & Conditions](#) and the [Ethical guidelines](#) still apply. In no event shall the Royal Society of Chemistry be held responsible for any errors or omissions in this Accepted Manuscript or any consequences arising from the use of any information it contains.

## RESEARCH ARTICLE

## Redox-Neutral electrochemical Diazo Coupling: Controlled Synthesis of Olefins and Azines via modulating reaction conditions

Abinash Mohapatra<sup>a</sup>, and Vikas Tyagi<sup>\*a</sup>Received 00th January 20xx,  
Accepted 00th January 20xx

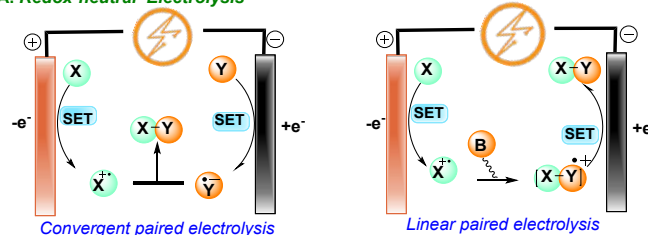
DOI: 10.1039/x0xx00000x

We report a metal-free, linear paired redox-neutral electrochemical diazo coupling that enables the controllable synthesis of olefins and azines by modulating reaction conditions. The protocol exhibits a broad substrate scope, delivering desired products in good yields and diastereoselectivities. Mechanistic investigations, including control experiments and cyclic voltammetry studies, support a cathodically initiated radical-anion formation pathway.

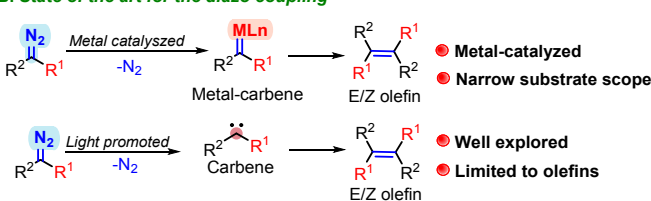
The conventional electrochemical synthesis generally operates at a single electrode, while the counter electrode performs a complementary process that often produces by-products. As a result, the overall transformation is inherently biased toward either oxidation or reduction, depending on where the synthetically relevant chemical reaction occurs. In contrast, redox-neutral electrochemical synthesis offers a distinct, more efficient paradigm in which both anodic and cathodic processes contribute to product formation.<sup>1</sup> As a result, each electrode participates in a coordinated, synthetically meaningful manner, enabling simultaneous oxidation and reduction within a single system and thereby maximizing efficiency. Moreover, redox-neutral electrochemical transformations are generally achieved through two distinct strategies: convergent and linear paired electrolysis.<sup>2</sup> In the convergent approach, intermediates generated separately at the anodic and cathodic sites subsequently combine to form the desired product (Scheme 1A). By contrast, linear paired electrolysis involves stepwise activation of a single substrate, simplifying the overall process (Scheme 1A). Although significant advances have been made in electrochemical methods that operate at individual electrodes, the development of redox-neutral processes, particularly for the synthesis of high-value organic molecules, remains relatively unexplored. To date, only a limited number of redox-neutral electrochemical strategies for the synthesis of organic compounds have been reported.<sup>3</sup> On the other hand, controlling product selectivity in electrochemical synthesis has gained significant attention in recent years, as it can be finely tuned by varying operational parameters rather than relying solely on substrate design or reagents. In this context, parameters such as the electrolyte type, electrode material, solvent, applied potential or current, and cell configuration play an important role in directing reaction pathways.<sup>4</sup> By systematically modulating these parameters, it becomes possible to favour one product over another, enabling

switchable synthesis from the same set of starting materials. In recent years, several studies have mainly highlighted the effects of electrode materials and the nature of the electrolyte on electrochemical reaction outcomes, especially on product selectivity.<sup>5</sup> In this context, Chiba and co-workers demonstrated the influence of electrode materials on the oxygen-mediated

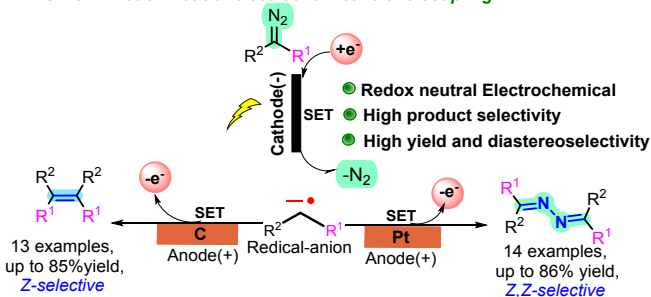
## A. Redox-neutral Electrolysis



## B. State of the art for the diazo coupling



## C. This work: Redox-neutral electrochemical diazo coupling



<sup>a</sup> Department of Chemistry and Biochemistry, Thapar Institute of Engineering and Technology, Patiala-147004, Punjab, India.

<sup>b</sup> Email: vikas.tyagi@thapar.edu

† Footnotes relating to the title and/or authors should appear here.

functionalization of styrene, with platinum electrodes favour the formation of tetrahydrofuran derivatives.<sup>5a</sup>

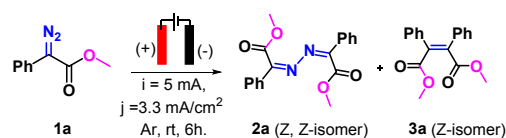
Next, Diazo compounds are highly versatile building blocks in organic synthesis, enabling a broad range of chemical transformations, such as X–H carbene insertions (X = C, N, O, S, Si, B, etc.), C–C coupling, Wolff rearrangement, and cyclopropanation<sup>6</sup> In recent years, diazo coupling has emerged as an efficient and versatile strategy for the construction of both symmetrical and unsymmetrical olefins and azines. The first carbene homo coupling reaction using diazo compounds was reported by Grundmann in 1938,<sup>7</sup> marking a significant milestone in diazo chemistry. Later on, the reductive coupling of diazo compounds through the terminal nitrogen to synthesize azines was reported by Pickett in 1982.<sup>8</sup> Since then, numerous catalytic methods have been developed to facilitate carbene homo/cross-coupling reactions using diazo compounds. In this context, transition-metal catalysts such as rhodium, silver, gold, cobalt, and copper have been widely applied,<sup>9</sup> whereas, more recently, photocatalytic strategies have emerged as greener alternatives to homo- and cross-coupling reactions of diazo compounds (Scheme 1B).<sup>10</sup> Previously, Tilley's group reported Co(I) catalysis for the intermolecular homo coupling of aryl diazo esters to yield both azine and olefin derivatives selectively using a cobalt-based catalyst.<sup>11</sup> Subsequently, Sivasankar and co-workers reported a Cu(I)/phosphine–Grignard system that favours the selective synthesis of azine derivatives along with olefin formation.<sup>12</sup> However, these approaches still suffer from notable limitations, including the need for transition metal catalysts, limited substrate scope, and a primary focus on a single class of products, either olefins or azines. Also, the light-catalyzed approaches are mainly restricted to olefin synthesis.

In addition, numerous electrochemical studies have reported the incidental formation of olefins or azines as by-products when diazo compounds are used as starting materials.<sup>13</sup> However, to the best of our knowledge, these observations have not been systematically developed into a controlled electrochemical strategy for the selective synthesis of either azines or olefins.<sup>14</sup> Considering the synthetic importance of diazo coupling in accessing the valuable tetrasubstituted olefins and azines, along with the inherent advantages of electrochemical methods in enabling product control without the need for external reagents or catalysts, we herein report a linear paired redox-neutral electrochemical coupling of diazo compounds that allows tuneable and selective synthesis of azines and olefins through simple modulation of reaction conditions (Scheme 1C).

We began our investigation by screening reaction conditions for the electrochemical coupling of phenyl diazoester (**1a**) as a model substrate (Table 1 and Table S1). Initially, electrolysis of 0.1 mmol of (**1a**) in acetonitrile (MeCN), using 0.04 M nBu<sub>4</sub>NPF<sub>6</sub> as the supporting electrolyte and Pt/Pt electrodes at room temperature, afforded azine (**2a**) and olefin (**3a**) in 31 % and 15 % yields, respectively, with excellent diastereomeric excess (Table 1, entry 1). To improve conversion and product selectivity between azine (**2a**) and olefin (**3a**), we systematically varied the electrolyte, electrode material, and solvent (representative data in Table 1; full details in Table S1). Notably, replacing nBu<sub>4</sub>NPF<sub>6</sub> with nBu<sub>4</sub>NBr significantly improved the reaction outcome, increasing the yield of azine (**2a**) with good diastereoselectivity (Table 1, entry 2), whereas ammonium iodide and tetrafluoroborate salts were less effective (Table S1, entries 3 and 4). A pronounced electrode effect was observed when Pt/Pt electrodes were replaced with C/C electrodes under otherwise

identical conditions (Table 1, entry 3). In this case, selectivity shifted toward olefin formation, with (**3a**) as the major product and only trace amounts of azine (**2a**) detected. Further variation of the supporting electrolyte while using C/C electrodes consistently afforded olefin (**3a**) as the major product with very high diastereomeric excess, underscoring the decisive role of electrode material in dictating the reaction pathway (Table 1, entry 4 and Table S1, entries 6-8).

**Table 1.** Optimization of the reaction conditions for the control synthesis of azine (**2a**) and olefin (**3a**).



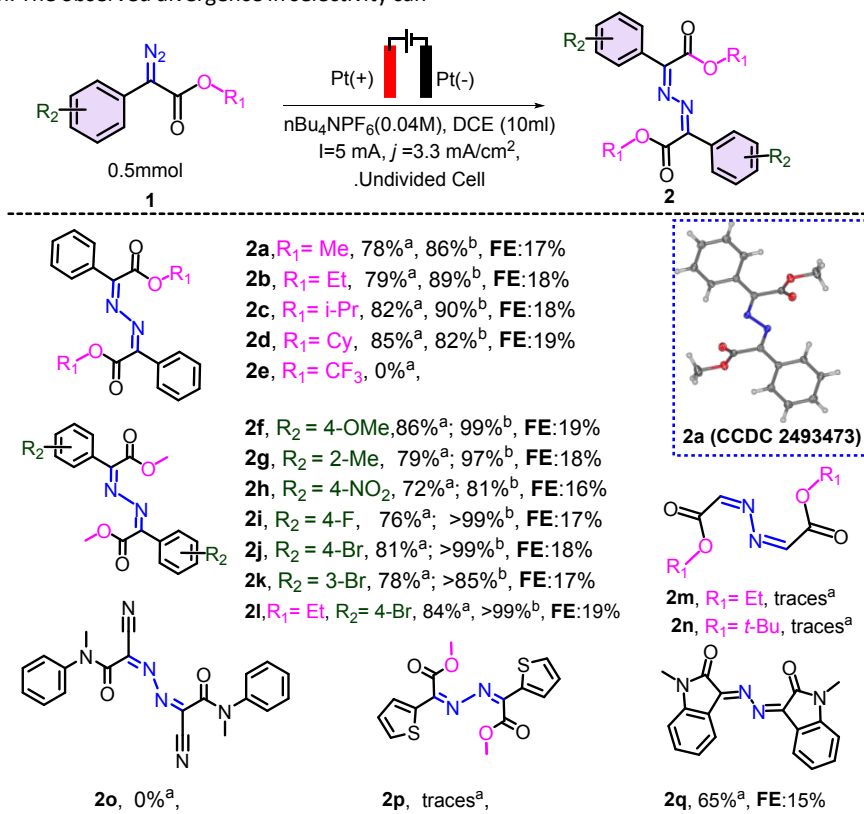
Entry	Electrolyte	(+) / (-)	%Yield <sup>b</sup> ( <b>2a</b> ), (%de) <sup>c</sup>	%Yield <sup>b</sup> ( <b>3a</b> ), (%de) <sup>c</sup>
1	Bu <sub>4</sub> NPF <sub>6</sub>	Pt/Pt	31%, (99%)	15%, (90%)
2	Bu <sub>4</sub> NBr	Pt/Pt	78%, (99%)	20%, (97%)
3	Bu <sub>4</sub> NBr	C/C	8%, (80%)	70%, (99%)
4	Bu <sub>4</sub> NI	C/C	12%, (90%)	67%, (98%)
5	Bu <sub>4</sub> NPF <sub>6</sub>	Pt/Pt	95%, (86%)	0%
6	Bu <sub>4</sub> NBr	Pt/Pt	90%, (94%)	4%, (80%)
7	Bu <sub>4</sub> NBF <sub>4</sub>	Pt/Pt	62%, (96%)	15%, (50%)
8	Bu <sub>4</sub> NPF <sub>6</sub>	C/C	12%, (62%)	66%, (56%)
9	Bu <sub>4</sub> NBr	C/C	0%	83%, (99%)
<sup>d</sup> 10	Bu <sub>4</sub> NPF <sub>6</sub>	Pt/Pt	0%	0%
<sup>e</sup> 11	Bu <sub>4</sub> NPF <sub>6</sub>	Pt/Pt	0%	0%

<sup>a</sup>All entries were carried out under identical constant-current conditions with **1a** (0.1 mmol, 17.6 mg) in 2 mL of solvent containing 0.04 M electrolyte. Entries 1–4 were performed in acetonitrile (MeCN), entries 5–9 in 1,2-dichloroethane (DCE), unless otherwise noted. <sup>b</sup>Determined by HPLC, <sup>c</sup>Diastereomeric excess (% de) determined by HPLC; <sup>d</sup>no electricity, <sup>e</sup>open air

Moreover, solvent screening revealed that chlorinated solvents markedly enhance azine selectivity when combined with Pt/Pt electrodes. In 1,2-dichloroethane (DCE), both nBu<sub>4</sub>NPF<sub>6</sub> and nBu<sub>4</sub>NBr afforded azine (**2a**) in more than 90% yield with suppression of olefin formation, whereas nBu<sub>4</sub>NI and nBu<sub>4</sub>NBF<sub>4</sub> provided modest yields of azine (**2a**), along with minor formation of olefin (**3a**) (Table 1, entries 5–7, and Table S1, entries 9,10,12). Moreover, the electrode-dependent selectivity observed in MeCN was retained in DCE; switching from Pt/Pt to C/C electrodes inverted the product distribution, favoring the olefin pathway irrespective of the supporting electrolyte (Table 1, entry 8-9, and Table S1, entries 13–14). In contrast, the highly polar protic solvent hexafluoroisopropanol (HFIP) proved detrimental, leading to low conversions and diminished stereocontrol, likely because strong solvation and hydrogen bonding interfere with the productive radical-anion pathway (Table S1, entries 17-18). Further, control experiments highlighted the crucial role of electrochemical activation and an inert atmosphere. In the absence of applied current, no formation of azine (**2a**) or olefin (**3a**) was observed, demonstrating that the transformation does not proceed in the absence of electricity (Table 1, entry 10). Likewise, conducting the reaction under open-air conditions led to rapid oxidation of (**1a**) to methyl 2-oxo-2-phenylacetate, with no formation of coupling products (**2a**) and (**3a**) (Table 1, entry 11). Moreover, at 3 mA (Table S1, entries 24), the lower current density reduces the rate of electron

transfer, resulting in a lower steady-state concentration of the key radical-anion intermediate (B), which slows the overall coupling and allows competing decomposition pathways to erode both yield and stereocontrol. While, at 10 mA (Table S1, entry 24), the increased current density accelerates the generation of radical-anion intermediates, but the higher flux of reactive species promotes non-selective coupling pathways and over-reduction, diminishing both yield and diastereoselectivity.<sup>15</sup> The optimal performance at 5 mA reflects a balance between sufficient radical-anion generation for productive coupling and controlled reaction kinetics that maintain high stereochemical fidelity with 0.1 mmol of substrate. Collectively, these studies demonstrate that the electrode material is the primary determinant of product selectivity. Consequently, Pt/Pt electrodes favor azine formation, whereas C/C electrodes promote olefin formation. The observed divergence in selectivity can

be rationalized through an electrode-controlled radical-anion mechanism, as reported in the literature.<sup>15,51</sup> Platinum electrodes, characterized by rapid heterogeneous electron transfer, promote faster formation of intermediate B, and stronger adsorption of  $\pi$ - and N-containing intermediates, favor a surface-confined inner-sphere pathway that promotes N–N bond formation, leading to azine 2a.<sup>17</sup> In contrast, carbon electrodes predominantly operate via outer-sphere electron transfer, thereby increasing the lifetime of radical-anion intermediate B in solution and facilitating pathways leading to olefin 3a.<sup>18</sup> Furthermore, solvent polarity and electrolyte nature primarily influence ion pairing, double-layer organization, and overall reaction efficiency, thereby modulating diastereoselectivity and the relative contribution of competing pathways without altering the underlying radical-anion manifold.<sup>19</sup>



**Scheme 2:** Substrate scope of electrochemical azine formation; All the reactions were performed under a constant current of 5 mA, room temperature, under argon atmosphere, 6 h, total charge passed ( $Q$ ) = 2.23 F/mol; <sup>a</sup>isolated yield, <sup>b</sup>de (diastereomeric excess of Z-Z isomer), Faradaic Efficiency (FE).

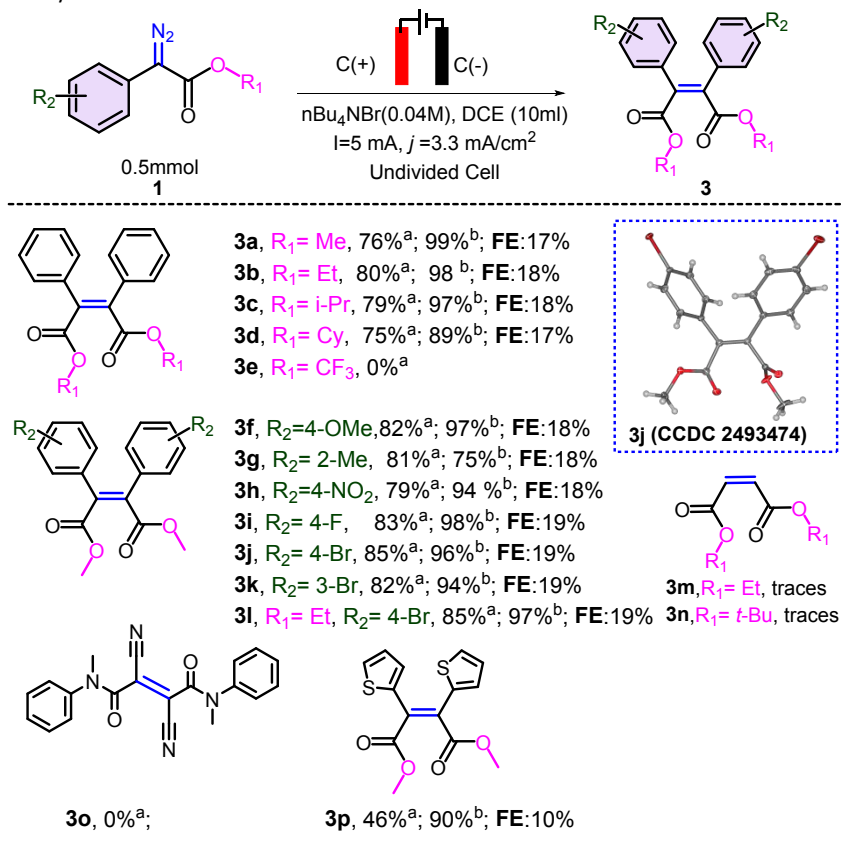
After optimizing the electrochemical parameters for selective azine and olefin formation (entries 8 and 14, Table 1), we next explored the substrate scope using the optimized conditions that favour azine formation (Scheme 2). Initially, the effect of different ester functionalities on the reaction outcome was examined. In this context, phenyl diazoesters bearing alkyl groups such as Me, Et, *i*-Pr, and cyclohexyl were smoothly converted, affording the desired azine products (**2a–2d**) in 78–85% isolated yields, with high product selectivity over olefin formation and excellent diastereomeric excess (up to 90% de). In contrast, the trifluoromethyl-substituted ester afforded only trace amounts of azine (**2e**) along with extensive decomposition of the starting material, indicating that the  $\text{CF}_3$  group destabilizes the diazo intermediate and promotes premature loss of  $\text{N}_2$ . Next, the effect of aryl substitution was investigated. Subsequently, electron-donating groups, such as a 4-OMe substituent, were well tolerated, affording the desired azines (**2f**) in

up to 86% yield. In comparison, the 2-Me-substituted analogue gave a slightly lower yield of product (**2g**), likely due to increased steric congestion at the reactive center. Next, electron-withdrawing groups such as 4- $\text{NO}_2$  were also found to be compatible but afforded reduced yields of azine (**2h**) and a decrease in diastereomeric excess, likely reflecting diminished stability of the radical-anion intermediate. Further, halogen substituents (4-F and 4-Br) had minimal impact on reactivity or selectivity, delivering the azines (**2i–2j**) in comparable yields and very high diastereomeric excess. Additionally, 3-bromo meta substitution (**2k**) was also tolerated, affording the azine in 78% yield with up to 85% diastereomeric excess. Also, 4-bromo substitution on the phenyl ring of diazo ester in combination with ethyl ester was well tolerated and obtained the desired product (**2l**) in 84% yield and more than 99% de. Beyond aryl diazoesters, when the aliphatic  $\alpha$ -diazo esters were tested, only trace amount of azine (**2m**, **2n**) was formed, consistent with the lower

Downloaded from https://www.rsc.org/journals by University of Cambridge on 06/20/2026 11:43:14 AM. This article is licensed under a Creative Commons Attribution-NonCommercial 3.0 Unported Licence.

stability of the cathodically generated radical-anion in the absence of conjugation. Methyl 2-diazo-2-(thiophen-2-yl) acetate also afforded only traces of azine (**2p**), whereas the amide diazo 2-cyano-2-diazo-N-methyl-N-phenylacetamide (**2o**) did not yield any product. In contrast, a heteroaromatic isatin-derived diazo compound performed well, furnishing the azine (**2q**) in 65% isolated yield with excellent stereocontrol; thereby underscoring the role of extended conjugation in stabilizing the key radical anion intermediate.

Further, the modest Faradaic efficiencies observed are consistent with a catalytic electron-initiation pathway, which a sub-stoichiometric amount of charge triggers radical formation, which then propagates chemically.<sup>20</sup> The stereochemical assignment of the major product was confirmed by single-crystal X-ray analysis of (**2a**), which revealed exclusive formation of the Z, Z-configured azine (**Figure S12**).



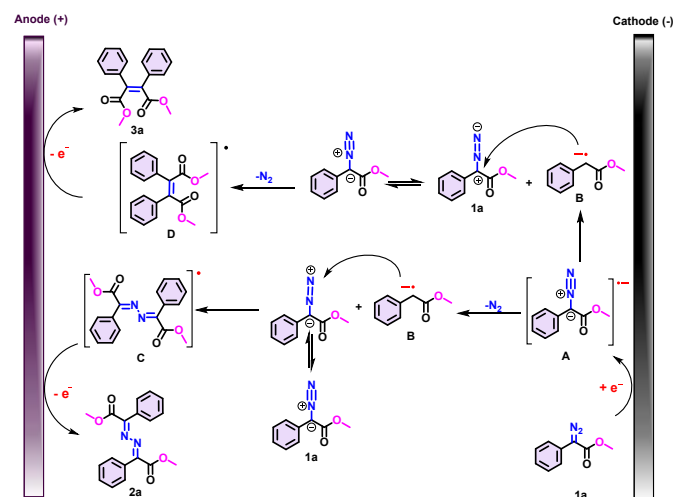
**Scheme 3:** Substrate scope of electrochemical olefin formation; All the reactions were performed under a constant current of 5mA, room temperature, under argon atmosphere, 6 h, total charge passed (Q) = 2.23 F/mol; <sup>a</sup>isolated yield, <sup>b</sup>de (diastereomeric excess of Z-Z isomer), Faradaic Efficiency (FE).

In the second stage of our study, we examined the substrate scope for the selective formation of olefinic products under the optimized conditions. In this context, phenyl diazo esters containing Me, Et, n-Pr, or cyclohexyl ester groups gave the corresponding Z-olefins (**3a–3d**) in good yields, i.e., 75–80%, with consistently high diastereoselectivity (%de up to 99%). Next, the scope of substitutions on the phenyl ring of phenyl diazo ester was screened. Subsequently, electron-donating groups (4-OMe and 2-Me) were well tolerated and gave the desired olefins (**3f**, **3g**) in good yields; however, diastereoselectivity was slightly dropped in the case of 2-methyl substitution. An electron-withdrawing substituent (4-NO<sub>2</sub>) also performed efficiently, delivering (**3h**) in good yield (79%) with good diastereoselectivity (% de = 94%). Moreover, halide substituents such as 4-F and 4-Br had a negligible impact on either yield or stereocontrol, furnishing the corresponding olefin products (**3i–3j**) in good yields and with high diastereoselectivity. Additionally, 3-bromo meta substitution (**3k**) was also well tolerated, affording the corresponding olefin in 82% yield with 94% diastereomeric excess. Further, 4-Br substitution in combination with ethyl ester gave the corresponding product (**3l**) in 85% isolated yield and 97% diastereomeric excess. Beyond aryl diazoesters, aliphatic α-diazo

esters such as (**3m**) & (**3n**) were unreactive under the electrochemical conditions, and only a trace of olefin product was observed, which might be due to the lower stability of the radical-anion intermediate in the absence of aryl groups. The amide diazo 2-cyano-2-diazo-N-methyl-N-phenylacetamide (**3o**) did not react, whereas in the case of Methyl 2-diazo-2-(thiophen-2-yl) acetate, the product (**3p**) was obtained in 46% yield with 90% de. The stereochemical assignments of the major and minor isomers of **3j** were confirmed by single-crystal X-ray diffraction (**Figure S13–S14**).

Downloaded from https://www.rsc.org/journals by University of Cambridge on 06/20/2026 11:43:14 AM. This article is licensed under a Creative Commons Attribution-NonCommercial 3.0 Unported Licence.





**Scheme 4.** Proposed mechanistic pathways for the electrochemical coupling of phenyl diazo ester (**1a**) leading to olefin and azine products

Based on previous reports, a plausible mechanism for the electrochemical diazo coupling of phenyl diazo ester (**1a**) is proposed (Scheme 4). The reaction is initiated by single-electron transfer (SET) at the cathode, affording the diazo radical anion (**A**).<sup>21</sup> Further, stabilization of intermediate (**A**) by the adjacent carbonyl group facilitates extrusion of dinitrogen, generating a radical anion intermediate (**B**).<sup>22</sup> This radical-anion intermediate (**B**) displays ambiphilic reactivity, where the radical center favors coupling while the anionic component supports nucleophilic attack.<sup>23</sup> Next, the radical anion (**B**) undergoes nucleophilic attack on the carbon center of phenyl diazo ester (**1a**), followed by the single electron oxidation at the anode to furnish the final olefin product (**3a**). In the other pathway, intermediate (**B**) undergoes nucleophilic attack at the terminal nitrogen of a second phenyl diazo ester molecule (**1a**), furnishing the azine radical intermediate (**C**), which further oxidizes at the anode to provide the final azine product (**2a**), consistent with the established diazo coupling pathway.<sup>24,18b</sup> Overall, these findings highlight a dual mechanistic manifold in which cathodically generated radical anions participate in diazo-coupling transformations, with the orientation of nucleophilic attack playing a key role in determining product selectivity.

At more negative potentials, the current increases markedly, consistent with a follow-up chemical step and an overall EC-type process. On the reverse scan, only background anodic currents associated with the supporting electrolyte are observed. This sequence involves a cathodic reduction of phenyl diazo ester (**1a**), followed by an oxidation that regenerates it, thereby completing the electrochemical cycle.

Next, a cyclic voltammetry was employed to probe the redox behavior of phenyl diazo ester (**1a**) under two different conditions, *i.e.*, 0.1 M *n*Bu<sub>4</sub>NPF<sub>6</sub> in DCE (Figure 1a & b) and 0.1 M *n*Bu<sub>4</sub>NBr in DCE (Figure 1c & d) (A detailed discussion is given in the SI, Figure S3.)

To gain insight into the proposed reaction mechanism, cyclic voltammetry (CV) experiment was set up (Figure 1), in the presence of 0.1 M *n*Bu<sub>4</sub>NPF<sub>6</sub> in DCE, recorded with a platinum disk working electrode and a non-aqueous Ag/Ag<sup>+</sup> reference electrode, shows a pronounced irreversible cathodic wave with a peak potential at -2.1 V vs Ag/Ag<sup>+</sup>, which might be attributed to a one-electron reduction of (**1a**) to give the corresponding radical anion intermediate (**A**). The radical anion intermediate (**A**) then decomposes rapidly, losing

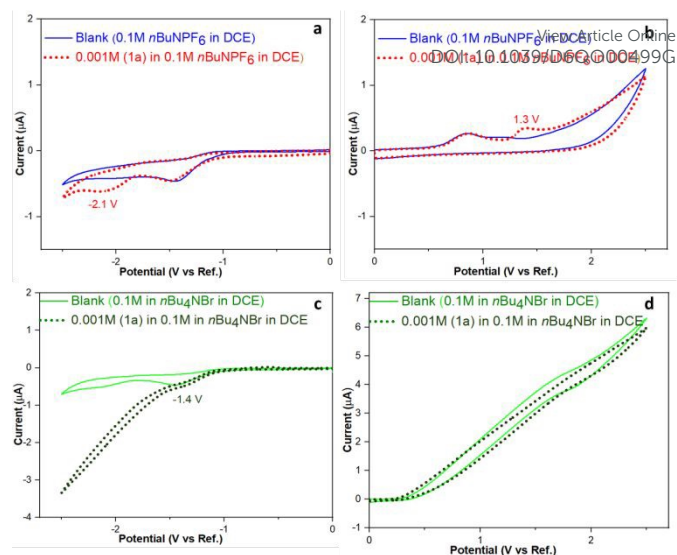
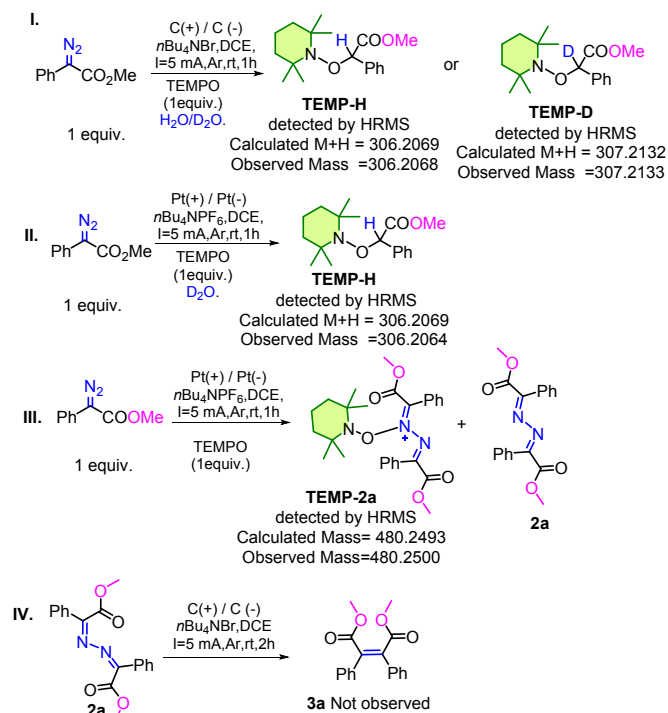


**Figure 1:** Cyclic voltammograms (CV) of 0.001M (**1a**) (a) Reduction Half under azine forming conditions (b) Reduction Half under olefin forming conditions in 0.1 M *n*Bu<sub>4</sub>NPF<sub>6</sub> in DCE. (c) Reduction Half under olefin conditions (d) oxidation half under olefin conditions in 0.1 M *n*Bu<sub>4</sub>NBr in DCE.

nitrogen to generate a carbanion (**B**). Further, a cyclic voltammetry experiment was conducted under reaction conditions used for the selective synthesis of olefin products, *i.e.*, phenyl diazoacetate (**1a**) in 0.1 M *n*Bu<sub>4</sub>NBr in dichloroethane (DCE). In this medium, a cathodic peak is observed at -1.4 V vs Ag/Ag<sup>+</sup>, which is not present in the blank electrolyte trace and is therefore assigned to the reduction of (**1a**) to radical anion (**A**). At more negative potentials, the current increases markedly, consistent with a follow-up chemical step and an overall EC-type process. On the reverse scan, only background anodic currents associated with the supporting electrolyte are observed. While the key cathodic features remain the primary evidence for the proposed radical-anion pathway. This sequence involves a cathodic reduction of phenyl diazo ester (**1a**), followed by an oxidation that regenerates it, thereby completing the electrochemical cycle.

To probe the radical-anion pathway, an experiment was set up in the presence of 1.0 equiv. of 2,2,6,6-tetramethyl-1-piperidinyloxy (TEMPO) using the reaction conditions (Table 1, entry 9) optimized for the selective formation of olefin products (Scheme 5-I). After 1 h, the mixture was quenched with H<sub>2</sub>O, and HR-MS showed a protonated TEMPO adduct (TEMP-H). Interestingly, quenching with D<sub>2</sub>O yielded the deuterated analogue (TEMP-D), suggesting that a radical and a concomitant anion, *i.e.*, intermediate B (Scheme 4), are generated. Further, to get information about the azine formation pathway, the azine-selective conditions (Table 1, entry 5) were examined in the presence of TEMPO. After 1 h, the mixture was quenched with H<sub>2</sub>O, and HRMS analysis revealed the formation of adduct (TEMP-H, Scheme 5-II). This experiment indicated that a radical anion intermediate (**B**) was formed during the azine formation pathway. Interestingly, adding TEMPO after 30 min of reaction progress, followed by quenching after an additional period of 10 minutes, produced both the azine product **2a** (*m/z* = 325.1185) and a TEMPO-**2a** adduct (*m/z* = 480.2500, Scheme 5-III), suggesting the formation of an azine radical intermediate (**C**) (Scheme 4). Finally, azine (**2a**) was subjected to the olefin-selective conditions (entry 9, Table 1); it remained unchanged (Scheme 5-IV), demonstrating that azine does not serve as a precursor to the olefin. In the end, we successfully performed a gram-scale synthesis. The reaction of substrate (**1b**) furnished the desired product (**3b**) in 74% isolated yield. Similarly, compound (**2c**) was obtained from (**1c**) in

77% isolated yield. However, the reaction took a little longer to complete (page S15-16 in SI). To further showcase the synthetic utility of the homocoupled products, we performed further transformation. In particular, the representative olefin (**3a**) was converted into the corresponding anhydride derivative<sup>18</sup>. This transformation underscores the value of the electrochemically generated olefins as versatile building blocks for constructing functionalized anhydride frameworks.



Scheme 5. Control experiments.

Next, computational analysis was undertaken to elucidate the intrinsic factors governing stereoselectivity across both the olefin and the azine (Figure 2). The calculations were focused on evaluating the inherent stabilities and stereochemical preferences of the neutral products formed after the electrochemical steps, without explicitly modeling the electrode electrolyte interface or the redox events, as commonly adopted in product-level mechanistic studies of electrochemical transformations. The geometries of the relevant isomeric products (**2a**), (**2a'**), (**3a**), and (**3a'**) were optimized using density functional theory (DFT) geometry optimizations using Gaussian16, and ORCA (version 5.0.3) (*More Computational details are provided in supporting information*). The calculated free-energy differences reveal a consistent intrinsic thermodynamic bias that rationalizes the experimentally observed selectivity across both reaction manifolds. For the azine products, isomer (**2a'**) is predicted to be less stable than (**2a**) by 3.3 kcal/mol, a free-energy difference that corresponds to a strongly selective population bias at ambient temperature and is widely accepted as sufficient to account for stereochemical outcomes in organic reactions. Likewise, for the olefinic coupling products, the Z-isomer (**3a**) is calculated to be more stable than the corresponding E-isomer (**3a'**) by 3.6 kcal/mol. These energetic preferences arise from a balance of electronic and noncovalent interactions, including favorable  $\pi$ - $\pi$  stacking and dispersion effects that are selectively accessible in the preferred geometries and outweigh steric congestion, consistent with established mechanistic paradigms for conjugated olefins.

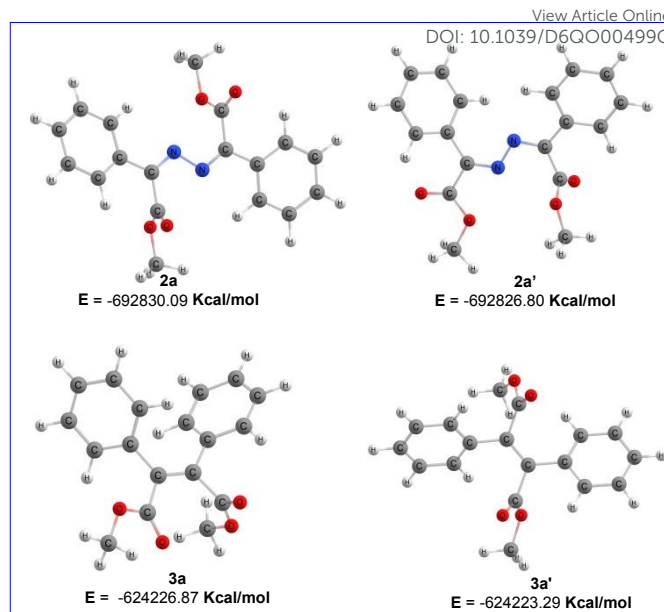


Figure 2: Optimized geometries and the corresponding electronic Energy of **2a**, **2a'**, **3a**, and **3a'**.

In summary, we have developed a transition-metal-free, linear-paired redox-neutral electrochemical platform for the switchable homo-coupling of aryl diazoesters. The protocol exhibits a broad substrate scope, tolerating a range of ester groups, electron donating and with drawing groups, along with halides, delivering products in good to excellent yields along with high diastereoselectivities. Mechanistic investigations, supported by CV and control experiments, revealed a radical-anion pathway in which the electrode interface directs selective product formation. Thus, this study provides an example of a redox-neutral electrochemical process in which product selectivity between two classes of compounds can be rationally controlled by tuning electrochemical parameters rather than changing catalysts or substrates.

## Conflicts of interest

The authors declare no conflict of interest.

## Data availability

\*SI Supporting Information: The supporting information contains experimental procedures, additional reaction optimization details, detailed discussion of cyclic voltammetry studies, Energy optimization for E- and Z-diastereoisomers, compound characterization data, and <sup>1</sup>H and <sup>13</sup>C-NMR spectra.

## Acknowledgements

We acknowledge financial support from the Department of Biotechnology, India (BT/PR55062/BSA/33/294/2024) and Thapar Institute of Engineering and Technology (TIET)–Virginia Tech CEEMS (TIET/CEEMS/Regular/2022/042). We thank DST-FIST (SR/FST/CS-II/2018/69) for HRMS facilities at TIET and Suraj Kumar Agrawalla (NISER, Bhubaneswar) for access to the Single Crystal X-ray Diffraction (SCXRD) facility.

## Notes and references

Downloaded from https://www.rsc.org/journals by University of Cambridge on 06/06/2024 14:43:14 AM. This article is licensed under a Creative Commons Attribution-NonCommercial 3.0 Unported Licence.

- 1  
2  
3  
4  
5  
6  
7  
8  
9  
10  
11  
12  
13  
14  
15  
16  
17  
18  
19  
20  
21  
22  
23  
24  
25  
26  
27  
28  
29  
30  
31  
32  
33  
34  
35  
36  
37  
38  
39  
40  
41  
42  
43  
44  
45  
46  
47  
48  
49  
50  
51  
52  
53  
54  
55  
56  
57  
58  
59  
60
- 1 (a) Lee, K. M., Jang, J. H., Balamurugan, M., Kim, J. E., Jo, Y. I. and Nam, K. T., Redox-neutral electrochemical conversion of CO<sub>2</sub> to dimethyl carbonate, *Nature Energy*, 2021, **6**, 733–741;(b) Mo, Y., Lu, Z., Rughoobur, G., Patil, P., Gershenfeld, N., Akinwande, A. I., Buchwald, S. L. and Jensen, K. F., Microfluidic electrochemistry for single-electron transfer redox-neutral reactions, *Science*, 2020, **368**, 1352–1357.
- 2 (a) Nie, L., Yang, J., Liu, Z., Zhou, S., Chen, S., Qi, X., Lei, A. and Yi, H., Linear paired electrolysis enables redox-neutral (3 + 2) annulation of benzofuran with vinyl diazo compounds, *Journal of the American Chemical Society*, 2024, **146**, 31330–31338;(b) Wu, T. and Moeller, K. D., Organic electrochemistry: expanding the scope of paired reactions, *Angew. Chem.*, 2021, **133**, 12993–13000;(c) Sbei, N., Hardwick, T. and Ahmed, N., Green chemistry: electrochemical organic transformations via paired electrolysis, *ACS Sustainable Chemistry & Engineering*, 2021, **9**, 6148–6169.
- 3 (a) Chen, Y., Ye, Y., Zhou, H., Zhang, Y., Fan, J., Sun, H., Chen, G., Wang, Y., Zhou, Y. and Zhang, D., Redox-neutral electrochemical cis-cyclopropanation of alkenes with sulfoxonium ylides, *Angew. Chem.*, 2026, **138**, e7024568;(b) Kong, K., Li, A. Z., Wang, Y., Shi, Q., Li, J., Ji, K. and Duan, H., Electrochemical carbon–carbon coupling with enhanced activity and racemate stereoselectivity by microenvironment regulation, *Nature Communications*, 2023, **14**, 6925.
- 4 (a) Corbin, N., Junor, G. P., Ton, T. N., Baker, R. J. and Manthiram, K., Toward improving the selectivity of organic halide electrocarboxylation with mechanistically informed solvent selection, *Journal of the American Chemical Society*, 2023, **145**, 1740–1748;(b) Mathison, R., Rani, E., Rose, A. M., Prendi, F., Bloomquist, C. K. and Modestino, M. A., Controlling selectivity in electrochemical conversion of organic mixtures through dynamic control of electrode microenvironments, *Journal of the American Chemical Society*, 2025, **147**, 37576–37586;(c) Jing, Q. and Moeller, K. D., From molecules to molecular surfaces: exploiting the interplay between organic synthesis and electrochemistry, *Accounts of Chemical Research*, 2019, **53**, 135–143.
- 5 (a) Imada, Y., Okada, Y., Noguchi, K. and Chiba, K., Selective functionalization of styrenes with oxygen using different electrode materials: olefin cleavage and synthesis of tetrahydrofuran derivatives, *Angewandte Chemie International Edition*, 2019, **58**, 125–129;(b) Li, A., Li, J., Yin, M., Zhang, Q., Chen, J., Pi, B., Bao, M., Song, C., Shi, W., Yu, C. and Zhang, W., Potential-modulated selective electro-synthesis of azo-tetrazole energetic compounds via a Co<sub>2</sub>P nanowire-based cathode, *Inorganic Chemistry*, 2025, **64**, 16404–16412;(c) Corbin, N., Junor, G. P., Ton, T. N., Baker, R. J. and Manthiram, K., Toward improving the selectivity of organic halide electrocarboxylation with mechanistically informed solvent selection, *Journal of the American Chemical Society*, 2023, **145**, 1740–1748.
- 6 (a) F. Doraghi, P. Baghersahi, M. Ghasemi, M. Mahdavi and A. Al-Harrasi, Rhodium-Catalyzed Transformations of Diazo Compounds via a Carbene-Based Strategy: Recent Advances, *RSC Adv.*, 2024, **14**, 39337–39352. (b) Y. Xia, D. Qiu and J. Wang, Transition-Metal-Catalyzed Cross-Couplings through Carbene Migratory Insertion, *Chem. Rev.*, 2017, **117**, 13810–13889. (c) Z. Zhang and V. Gevorgyan, Visible Light-Induced Reactions of Diazo Compounds and Their Precursors, *Chem. Rev.*, 2024, **124**, 7214–7261. (d) Y. He, Z. Huang, K. Wu, J. Ma, Y.-G. Zhou and Z. Yu, Recent Advances in Transition-Metal-Catalyzed Carbene Insertion to C–H Bonds, *Chem. Soc. Rev.*, 2022, **51**, 2759–2852. (e) H. Keipour, V. Carreras and T. Ollevier, Recent Progress in the Catalytic Carbene Insertion Reactions into the Silicon–Hydrogen Bond, *Org. Biomol. Chem.*, 2017, **15**, 5441–5456.
- 7 Grundmann, C., Über die Zersetzung der Diazoketone, *Justus Liebigs Annalen der Chemie*, 1938, **536**, 29–36. View Article Online  
DOI: 10.1039/D6QO00499G
- 8 Pickett, C. J., Tolhurst, J. E., Copenhaver, A., George, T. A. and Lester, R. K., Electrochemical carbon–carbon coupling of diazomethane ligands, *Journal of the Chemical Society, Chemical Communications*, 1982, **18**, 1071–1072.
- 9 (a) Del Zotto, A., Baratta, W., Verardo, G. and Rigo, P., Functionalised cis-alkenes from the stereoselective decomposition of diazo compounds, catalysed by [RuCl(η<sup>5</sup>-C<sub>5</sub>H<sub>5</sub>)(PPh<sub>3</sub>)<sub>2</sub>], *European Journal of Organic Chemistry*, 2000, **2000**, 2795–2801;(b) Hodgson, D. M. and Angrish, D., Highly chemo- and stereoselective intermolecular coupling of diazoacetates to give cis-olefins by using Grubbs second-generation catalyst, *Chemistry – A European Journal*, 2007, **13**, 3470–3479;(c) Rivilla, I., Sameera, W. M. C., Alvarez, E., Díaz-Requejo, M. M., Maseras, F. and Pérez, P. J., Catalytic cross-coupling of diazo compounds with coinage metal-based catalysts: an experimental and theoretical study, *Dalton Transactions*, 2013, **42**, 4132–4138;(d) Wu, C. H., Chu, J. H., Chou, C. H., Lin, P. C., Ong, C. W. and Chiang, C. M., Ester-carbene and its dimerization with exclusive cis-selectivity on a silver surface, *The Journal of Physical Chemistry C*, 2022, **126**, 2482–2492;(e) Yao, X., Wang, T. and Zhang, Z., Gold(I)-catalyzed dimerization of 3-diazoindoles towards isoindigos, *European Journal of Organic Chemistry*, 2018, **2018**, 4475–4478;(f) Cheng, H., Yao, X., Yin, S., Wang, T. and Zhang, Z., Stereoselective synthesis of (E)-3-alkylideneoxindoles via gold(I)-catalyzed cross-coupling of 3-diazoindoles with diazoesters, *The Journal of Organic Chemistry*, 2020, **85**, 5863–5871;(g) Yruegas, S., Semproni, S. P. and Chirik, P. J., (PNP) cobalt-catalyzed olefination of diazoalkanes, *Organometallics*, 2022, **41**, 3138–3144;(h) Zhu, C., Xu, G., Ding, D., Qiu, L. and Sun, J., Copper-catalyzed diazo cross-/homo-coupling toward tetrasubstituted olefins and applications on the synthesis of maleimide derivatives, *Organic Letters*, 2015, **17**, 4244–4247.
- 10 (a) Zhao, S., Gao, N., Bao, N., Qian, M., Chen, Z. Y., Zhang, M. J. and Chen, X., Stereoselective synthesis of tetrasubstituted olefins via visible-light-promoted iodine-mediated homo-coupling of diazo compounds, *The Journal of Organic Chemistry*, 2022, **87**, 11826–11837;(b) Xiao, T., Mei, M., He, Y. and Zhou, L., Blue light-promoted cross-coupling of aryl diazoacetates and diazocarbonyl compounds, *Chemical Communications*, 2018, **54**, 8865–8868;(c) Ye, C., Cai, B. G., Lu, J., Cheng, X., Li, L., Pan, Z. W. and Xuan, J., Visible-light-promoted polysubstituted olefins synthesis involving sulfur ylides as carbene trapping reagents, *The Journal of Organic Chemistry*, 2020, **86**, 1012–1022.
- 11 Dong, Y., Lipschutz, M. I., Witzke, R. J., Panetier, J. A. and Tilley, T. D., Switchable product selectivity in diazoalkane coupling catalyzed by a two-coordinate cobalt complex, *ACS Catalysis*, 2021, **11**, 11160–11170.
- 12 Kuzhalmozhi Madarasi, P. and Sivasankar, C., Grignard reagent dictated copper(I) phosphines catalyzed reductive coupling of diazo compounds: the chemistry beyond carbene generation, *Applied Organometallic Chemistry*, 2022, **36**, e6522.
- 13 (a) Bera, S., Sen, S. and Maiti, D., Unveiling alternate electrode electrolysis in electro-photochemical and electro-organic syntheses, *Journal of the American Chemical Society*, 2024, **146**, 25166–25175;(b) He, Z., Zhao, W., Li, Y., Yu, Y. and Huang, F., Electrochemical S–H and O–H insertion reactions from thiols or salicylic acids with diazo esters, *Organic & Biomolecular Chemistry*, 2022, **20**, 8078–8082.
- 14 Wang, F., Gerken, J. B., Bates, D. M., Kim, Y. J. and Stahl, S. S., Electrochemical strategy for hydrazine synthesis: development and overpotential analysis of methods for

Downloaded on 06/20/2026 11:43:14 AM  
This article is licensed under a Creative Commons Attribution-NonCommercial 3.0 Unported Licence.



- oxidative N–N coupling of an ammonia surrogate, *Journal of the American Chemical Society*, 2020, **142**, 12349–12356.
- 15 (a) H. Wendt and V. Plzák, Addition reactions of anodically generated radicals to olefins: Part I. Theoretical discussion of the influence of alternative mechanisms and kinetic data on yields and selectivities of different electrocatalysis products, *Electrochim. Acta*, 1975, **20**, 181–188. (b) A. Wiebe, B. Riehl, S. Lips, R. Franke and S. R. Waldvogel, Unexpected high robustness of electrochemical cross-coupling for a broad range of current density, *Sci. Adv.*, 2017, **3**, eaao3920. (c) R. Mathison, R. Atwi, H. B. McConnell, E. Ochoa, E. Rani, T. Akashige, J. A. Röhr, A. D. Taylor, C. E. Avalos, E. S. Aydil, N. N. Rajput and M. A. Modestino, Molecular Processes That Control Organic Electrosynthesis in Near-Electrode Microenvironments, *J. Am. Chem. Soc.*, 2025, **147**, 4296–4307.
- 16 (a) Imada, Y., Okada, Y., Noguchi, K. and Chiba, K., Selective functionalization of styrenes with oxygen using different electrode materials: olefin cleavage and synthesis of tetrahydrofuran derivatives, *Angewandte Chemie International Edition*, 2019, **58**, 125–129; (b) Liu, C., Li, R., Zhou, W., Liang, Y., Shi, Y., Li, R. L., Ling, Y., Yu, Y., Li, J. and Zhang, B., Selectivity origin of organic electrocatalysis controlled by electrode materials: a case study on pinacols, *ACS Catalysis*, 2021, **11**, 8958–8967.
- 17 (a) Horn, E. J., Rosen, B. R. and Baran, P. S., Synthetic organic electrocatalysis: an enabling and innately sustainable method, *ACS Central Science*, 2016, **2**, 302–308; (b) Francke, R. and Little, R. D., Redox catalysis in organic electrocatalysis: basic principles and recent developments, *Chemical Society Reviews*, 2014, **43**, 2492–2521.
- 18 (a) Mathison, R., Rani, E., Rose, A. M., Prendi, F., Bloomquist, C. K. and Modestino, M. A., Controlling selectivity in electrocatalytic conversion of organic mixtures through dynamic control of electrode microenvironments, *Journal of the American Chemical Society*, 2025, **147**, 37576–37586; (b) Corbin, N., Junor, G. P., Ton, T. N., Baker, R. J. and Manthiram, K., Toward improving the selectivity of organic halide electrocarboxylation with mechanistically informed solvent selection, *Journal of the American Chemical Society*, 2023, **145**, 1740–1748.
- 19 (a) Bethell, D. and Parker, V. D., In search of carbene ion radicals in solution: reaction pathways and reactivity of ion radicals of diazo compounds, *Accounts of Chemical Research*, 1988, **21**, 400–407; (b) Baranton, S. and Bélanger, D., Electrochemical derivatization of carbon surface by reduction of in situ generated diazonium cations, *The Journal of Physical Chemistry B*, 2005, **109**, 24401–24410.
- 20 Imada, Y., Okada, Y. and Chiba, K., Investigating radical cation chain processes in the electrocatalytic Diels–Alder reaction, *Beilstein Journal of Organic Chemistry*, 2018, **14**, 642–647.
- 21 (a) Cheng, S. and Hawley, M. D., Electrochemical studies of diazoalkanes: the formation and decomposition of  $\text{Ph}_2\text{C}:\text{N}_2^-$  and  $\text{Ph}_2\text{C}:\text{N}_2^{2-}$ , *The Journal of Organic Chemistry*, 1986, **51**, 3799–3804; (b) Cowell, G. W. and Ledwith, A., Developments in the chemistry of diazo-alkanes, *Quarterly Reviews, Chemical Society*, 1970, **24**, 119–167; (c) Maiti, D., Saha, A., Guin, S., Maiti, D. and Sen, S., Unveiling catalyst-free electro-photochemical reactivity of aryl diazoesters and facile synthesis of oxazoles, imide-fused pyrroles and tetrahydro-epoxy-pyridines via carbene radical anions, *Chemical Science*, 2023, **14**, 6216–6225.
- 22 Bethell, D. and Parker, V., Dimers of the 9-diazafluorene anion radical and their behavior, *Journal of the American Chemical Society*, 1986, **108**, 895–900.
- 23 (a) Bethell, D., Gallagher, P., Self, D. P. and Parker, V. D., Cathodic oligomerisation of bis(diazo) compounds of the indenofluorene series: part 2. Kinetic and mechanistic aspects, *Journal of the Chemical Society, Perkin Transactions 2*, 1989, **8**, 1105–1109; (b) Jiao, J., Yan, Y., Ke, Q., Zhang, Y., Huang, H., Gao, Q., Liu, J. and Wang, X., Paired electrolysis enables decarboxylative coupling of alkenyl acids with diazo compounds, *Organic Chemistry Frontiers*, 2023, **10**, 2968–2975; (c) Zimmerman, H. E. and Somasekhara, S., The mechanism of the thermal decomposition reaction of azines, *Journal of the American Chemical Society*, 1960, **82**, 5865–5873.
- 24 (a) Francke, R. and Little, R. D., Redox catalysis in organic electrocatalysis: basic principles and recent developments, *Chemical Society Reviews*, 2014, **43**, 2492–2521; (b) Blanco, D. E., Atwi, R., Sethuraman, S., Lasri, A., Morales, J., Rajput, N. N. and Modestino, M. A., 2020. Effect of electrolyte cations on organic electrocatalysis: The case of adiponitrile electrochemical production. *Journal of The Electrochemical Society*, 167(15), p.155526; (c) Mathison, R., Rani, E., Rose, A. M., Prendi, F., Bloomquist, C. K. and Modestino, M. A., Controlling selectivity in electrocatalytic conversion of organic mixtures through dynamic control of electrode microenvironments, *Journal of the American Chemical Society*, 2025, **147**, 37576–37586.

**Data Availability Statement:**View Article Online  
DOI: 10.1039/D6QO00499G

The supporting information includes experimental procedures, additional reaction optimization details, a detailed discussion of cyclic voltammetry studies, Energy optimization for E- and Z-diastereoisomers, compound characterization data, and <sup>1</sup>H and <sup>13</sup>C NMR spectra.

1  
2  
3  
4  
5  
6  
7  
8  
9  
10  
11  
12  
13  
14  
15  
16  
17  
18  
19  
20  
21  
22  
23  
24  
25  
26  
27  
28  
29  
30  
31  
32  
33  
34  
35  
36  
37  
38  
39  
40  
41  
42  
43  
44  
45  
46  
47  
48  
49  
50  
51  
52  
53  
54  
55  
56  
57  
58  
59  
60

Downloaded on 06 June 2026 at 14:43:14 AM.  
This article is licensed under a Creative Commons Attribution-NonCommercial 3.0 Unported Licence.

